APJ, SUBMITTED
Preprint typeset using LATEX style emulateapj v. 11/12/01

NUCLEOSYNTHESIS IN BARYON-RICH OUTFLOWS ASSOCIATED WITH GAMMA-RAY BURSTS

SUSUMU INOUE[1,2], NOBUYUKI IWAMOTO[2], MANABU ORITO[2] AND MARIKO TERASAWA[2]
[1]Max-Planck-Institut für Astrophysik, Karl-Schwarzschild-Str. 1, Postfach 1317, 85741 Garching, Germany;
inouemu@mpa-garching.mpg.de
[2]Division of Theoretical Astrophysics, National Astronomical Observatory, 2-21-1 Osawa, Mitaka, Tokyo, Japan 181-8588;
iwamoto@th.nao.ac.jp, orito@th.nao.ac.jp, mariko@th.nao.ac.jp
ApJ, submitted

ABSTRACT

Robust generation of gamma-ray bursts (GRBs) implies the formation of outflows with very low baryon loads and highly relativistic velocities, but more baryon-rich, slower outflows are also likely to occur in most GRB central engine scenarios, either as "circum-jet winds" or "failed GRBs". Here we study the possibility of nucleosynthesis within such baryon-rich outflows by conducting detailed reaction network calculations in the framework of the basic fireball model. It is shown that high baryon load fireballs attaining mildly relativistic velocities can synthesize appreciable quantities of heavy neutron capture elements with masses up to the platinum peak and beyond. Small but interesting amounts of light elements such as deuterium and boron can also be produced. Depending on the neutron excess, the combination of high entropy, rapid initial expansion and gradual expansion at later times can cause the reaction flow to reach the fission regime, and its path can be intermediate between those of the *r*- and *s*-processes ("*n*-process"). The nucleosynthetic signature of these outflows may be observable in the companion stars of black hole binary systems and in the most metal-poor stars, potentially offering an important probe of the inner conditions of the GRB source. Contribution to the solar abundances for some heavy elements may also be possible. The prospects for further developments in various directions are discussed.

Subject headings: nuclear reactions, nucleosynthesis, abundances — gamma rays: bursts — stars: abundances

1. INTRODUCTION

Although many fundamental aspects of the nature of gamma-ray bursts (GRBs) remain mysterious, an essential requirement for any type of central engine to successfully generate a GRB is the formation of an ultrarelativistic outflow with bulk Lorentz factor $\Gamma \gtrsim 100$, so that the gamma-ray compactness problem can be avoided. This in turn implies the realization of a very low baryon load within the outflow, typically of isotropic equivalent mass $M \lesssim 10^{-4} M_\odot$. Regardless of its detailed properties, the conditions at the base of such an outflow should generically be radiation-dominated with very high entropy, high temperature ($\gtrsim$ MeV) and very high optical depth (see reviews by Piran 1999, Mészáros 2002).

The baryonic matter in the outflow is also expected to be enriched in neutrons, as the GRB engine is likely to involve some kind of collapsed stellar mass object, possibly with intense thermal neutrino emission (Fuller, Pruet & Abazajian 2000, Pruet, Woosley & Hoffman 2002b, Beloborodov 2002b). Matter that expands from MeV-temperature, neutron-rich conditions is known to be conducive to fusion of nuclei from initially free protons and neutrons. It is thus of interest to study the effects and implications of nucleosynthesis inside GRB outflows, which was the subject of several recent papers (Lemoine 2002, Pruet, Guiles & Fuller 2002a, Beloborodov 2002b). Production of nuclei turns out to be quite limited in the very high entropy ($\gtrsim 10^5 k_B$ per baryon) and extremely rapid expansion ($\lesssim 0.3$ msec) characteristic of GRB outflows, resulting only in the synthesis of some D and ^{4}He. The low total mass ejected per event and the low intrinsic event rate expected for GRBs imply that these products themselves are probably difficult to observe.

Besides the baryon-poor, ultrarelativistic outflow triggering the observable GRB emission, most GRB progenitors are also likely to give rise to associated outflows with much higher baryon-loading and lower velocities under different circumstances. Mounting evidence points to the high Γ GRB outflow being narrowly collimated into jets (Rhoads 2001, Frail et al. 2001). It is then highly probable that an outer, sheath-like wind of slower, baryon-rich material surrounds and coexists with the inner, fast jet. This may result either from launching conditions at the outflow base or from entrainment and mixing from the borders of the outflow, and can potentially convey total energies comparable to or even larger than the GRB jet itself (Levinson & Eichler 2000). Such "circum-jet winds" are anticipated not only in models comprising core collapse of massive stars (Zhang, Woosley & MacFadyen 2002, Aloy et al. 2002), but also in neutron star merger models (Janka & Ruffert 2001, Rosswog & Ramirez-Ruiz 2002) as well as more general accretion disk models in certain parameter regimes (Narayan, Piran & Kumar 2001). Their presence may be consistent with interpretations of the statistics of afterglow light curve breaks (Rossi, Lazzati & Rees 2002, Zhang & Mészáros 2002). Alternatively, baryon-rich outflows may occur without concomitant GRBs in various progenitor scenarios, when conditions are such that the baryon-loading process acts more thoroughly, or the mechanism for driving the GRB jet operates less efficiently (e.g. Narayan et al. 2001, Janka & Ruffert 2001, Woosley, Zhang & Heger 2002b). Such "failed GRBs" may have event rates higher than successful GRBs (Woosley et al. 2002b, Huang, Dai & Lu 2002). Perhaps some identification of failed GRBs can be made with observed "hypernovae" (i.e. explosions similar to ordinary supernovae but with much higher energies; Nomoto et al. 2002), the recently recognized class of X-ray flashes (Heise et al. 2001, Kippen et al. 2002), or with some hitherto undiscovered type of transient. Either as circum-jet winds or failed GRBs, these baryon-rich outflows (hereafter BROs) should be typified by lower entropy, slower expansion and higher ejecta mass compared to GRB jets, which are all more propitious from a nucleosynthesis viewpoint. [1]

The present work is an exploratory investigation of the different possibilities of nucleosynthesis within BROs associated with GRBs and their observational consequences. Besides the production of light elements, a particularly interesting issue is whether appreciable heavy element synthesis by neutron capture reactions can take place in such environments (Levinson & Eichler 1993, Janka & Ruffert 2001, Lemoine 2002, Pruet et al. 2002b). Elements heavier than Fe in the solar system are believed to arise from two distinct types of neutron capture processes, the *r*-process, for which the timescale of neutron capture is much faster than β-decay, and the *s*-process, for which the relation is vice-versa (e.g. Meyer 1994). The *s*-process proceeds with a nuclear reaction flow close to the line of β-stability, and is favored in situations with relatively low neutron abundances. Its main astrophysical site is thought to be asymptotic giant branch stars, a very different environment compared to GRB-BROs. For the *r*-process, the most widely discussed site is the neutrino-driven winds of core-collapse supernovae (e.g. Woosley et al. 1994, Takahashi, Witti & Janka 1994, Terasawa et al. 2002). Efficient operation of the *r*-process in such winds requires high entropy ($\sim 100-200 k_B$ per baryon), rapid expansion ($\sim 1-100$ msec) and high neutron excess ($Y_e \lesssim 0.43$ in terms of the electron fraction). GRB-BROs are intriguing in this regard, as their physical properties should be similar in a number of ways. The typical conditions in relativistic BROs can be even more extreme, but depending on the baryon load and other parameters, a successful *r*-process may also be possible. The *r*-process reaction flow in SN neutrino-driven winds is envisaged to occur far into the neutron-rich region close to the neutron dripline, whereby equilibrium is established between rapid neutron captures and their inverse reactions. After the flow terminates by consuming all available neutrons, β-decay to stable nuclei results in an abundance pattern with three peaks which reflect nuclei with neutron magic numbers at the *r*-process path.

This work investigates nucleosynthesis in GRB-BROs utilizing the simplified dynamical framework of the basic fireball model, but with detailed nuclear reaction networks (§2). Although this is a first step in a potentially broader problem, we find interesting results with regard to both light and heavy element production (§3). Some important observational implications of these nucleosynthetic products are pointed out, particularly for understanding the nature of the ill-understood GRB central engine (§4). We conclude with a discussion of various interesting possibilities for future studies (§5).

2. MODEL DESCRIPTION

2.1. *Dynamics*

We start with the simplest possible dynamical model: a spherical, adiabatic, thermally-driven flow that is freely expanding and in steady state (Paczynski 1986, 1990). The key parameters in this wind fireball model are the luminosity $L = 10^{52} L_{52}$erg s^{-1}, the initial radius $r_0 = 10^7 r_{0,7}$cm, and the dimensionless entropy $\eta = L/\dot{M}c^2$, where $\dot{M} \simeq 5.6 \times 10^{-3} \mathrm{M}_\odot \mathrm{s}^{-1} L_{52}\eta^{-1}$ is the baryon-loading rate. The initial bulk velocity is taken to be subrelativistic, $\Gamma_0 \simeq 1$. At the base of the outflow, the fireball plasma is radiation-dominated if $\eta \gtrsim 1$, its initial temperature is $k_B T_0 = \left(L/4\pi r_0^2 cag\right)^{1/4} \simeq 0.93\mathrm{MeV}\ L_{52}^{1/4} r_{0,7}^{-1/2}$ where a is the radiation constant and $g = 11/2$ the degrees of freedom including photons and electron-positron pairs, and its optical depth is very high due to the presence of the pairs. The entropy per baryon s is conserved in the flow and related to η and T_0 as $s/k_B = 4\eta m_N c^2/3kT_0 \simeq 1250\eta(T_0/1\mathrm{MeV})^{-1}$, where m_N is the nucleon mass (Fuller et al. 2000). The fireball starts to expand adiabatically and first undergoes an acceleration phase, where the bulk Lorentz factor Γ grows with radius as $\Gamma \propto r$ while the comoving temperature T falls as $T \propto r^{-1}$. This continues until the internal energy is fully converted to the bulk kinetic energy of the loaded baryons at the saturation radius $r_s = r_0\eta$. The fireball then enters a coasting phase with constant velocity $\Gamma = \eta$, where $T \propto r^{-2/3}$. These simple scalings derive from conservation of energy and rest mass along with adiabaticity and are strictly valid for $\Gamma \gg 1$. Lorentz transformations to the comoving frame give the profiles (trajectories) for the temperature T and baryon density ρ_b with respect to time t: for the acceleration phase ($t \leq t_s$),

$$T(t) = T_0 \exp(-t/t_{d0})$$
$$\rho_b(t) = \rho_{b,0} \exp(-3t/t_{d0}); \qquad (1)$$

for the coasting phase ($t \geq t_s$),

$$T(t) = \frac{T_0}{\eta}\left(1+\frac{t-t_s}{t_{d0}}\right)^{-2/3}$$
$$\rho_b(t) = \frac{\rho_{b,0}}{\eta^3}\left(1+\frac{t-t_s}{t_{d0}}\right)^{-2}. \qquad (2)$$

Here $t_{d0} = r_0/c \simeq 0.33$ msec is the initial light crossing time or dynamical time, $t_s = t_{d0}\ln\eta$ is the comoving saturation time, and $\rho_{b,0} = L/4\pi c^3 r_0^2 \eta \simeq 3.0 \times 10^5 \mathrm{g\ cm}^{-3}\eta^{-1}L_{52}r_{0,7}^{-2}$ is the initial baryon density. Note that $T = T_0\eta^{-1}(t/t_{d0})^{-2/3}$ and $\rho_b = \rho_{b,0}\eta^{-3}(t/t_{d0})^{-2}$ asymptotically for $t \gg t_s$. The trajectories above are in fact slightly modified by the effect of pair annihilation at $T \lesssim$ MeV, which is included in our calculations.

We see that the acceleration phase is characterized by an exponential expansion with e-folding time equal to the dynamical time at the outflow base (Fuller et al. 2000), whereas the coasting phase corresponds to a power-law expansion. A high η (low baryon load) fireball suffers from a long period of exponential drop in T and ρ in addition to a very high entropy, both severely hindering nucleosynthesis. In contrast, a low η (high baryon load) would allow the fireball to reach the power-law regime in a short time, where the more gradual decrease in T and ρ along with a lower entropy can greatly facilitate nucleosynthesis. We mention that these trajectories are virtually identical to those considered by Meyer (2002), except for the entropy which is lower in his case by an order of magnitude.

The description above is also applicable for an outflow confined to a conical channel so long as the opening half-angle $\theta \gtrsim \Gamma^{-1}$, in which case L and $\dot{M}$ should be interpreted as isotropic equivalent quantities. Flows which are strongly collimated, e.g. by external pressure gradients, would possess somewhat different scalings of physical variables with radius (Lemoine 2002, Beloborodov 2002b). Note that when compared to the narrow GRB jets, the BROs may inherently have a much wider geometry (Levinson & Eichler 2000), so that the present formulation may be useful even for modest Lorentz factor flows.

[1] Such phenomena are sometimes called “dirty fireballs” in the GRB literature, but this term is avoided here, as these outflows can be aesthetically appealing for nucleosynthesis.

As is apparent from the above arguments and also verified by actual calculations below, the lower the value of η, the more advantageous it is for nucleosynthesis. This is in terms of both the reaction flow to heavier nuclei and the total product mass. However, the above dynamical description must be modified if $\eta \lesssim 1$, i.e. the baryon load is sufficiently large that the fireball becomes nonrelativistic. Here we will limit ourselves to the relativistic scalings while imposing a lower limit of $\eta = 2$, a mildly relativistic fireball, which corresponds to total baryon mass $M_b = 2.8 \times 10^{-2} \mathrm{M}_\odot$ for total outflow energy $E = 10^{53}$erg. This is on two accounts. First, the physical regime of completely non-relativistic flows would be rather distinct from the high η GRB fireballs, and their actual properties, if they occur, are more uncertain. Second, for relatively baryon-free progenitor models such as neutron star mergers (Janka & Ruffert 2001) or possibly supranovae (Vietri & Stella 1998), $M_b \simeq 10^{-2} \mathrm{M}_\odot$ may be a reasonable upper bound to the potential amount of baryon contamination. As the assumption of free expansion should also suit these scenarios, the simple formulation employed here may be an adequate approximation for such classes of models. Cases of much higher baryon loading can happen, e.g. in the collapsar models, but this will be considered elsewhere. Various other effects that can be important for realistic GRB-BRO dynamics are touched upon in §5.

2.2. *Microphysics*

A critical quantity influencing the nuclear composition of baryonic matter is the neutron excess, commonly described in terms of the electron fraction $Y_e = (n_{e^-} - n_{e^+})/n_b$, i.e. the net number of electrons per baryon. The value of Y_e at the base of the outflow should be predictable if reliable physical models of the central engine can be constructed, but this is currently a difficult task. The material in the collapsing cores of massive stars typically have $Y_e \lesssim 0.5$, while material near the surfaces of cold neutron stars have $Y_e \simeq 0.1$. However, these can be significantly altered by capture of electrons (positrons) as well as electron-type neutrinos (antineutrinos) on protons (neutrons) during the course of the central engine evolution. The black hole accretion disk model evaluations by Pruet et al. (2002b) give numbers ranging from $Y_e \lesssim 0.1$ to $Y_e \gtrsim 0.5$ at the innermost edge of the disk, depending on parameters such as the viscosity, accretion rate, mass and angular momentum of the central black hole. Models invoking fireball formation in the envelopes of supermassive stars can instead be proton-rich, $Y_e \lesssim 1$ (Fuller & Shi 1998). In view of these uncertainties, we will treat Y_e as an additional free parameter in this work. Except when $T_0 \gg$ MeV, electron/positron captures within the fireball will not be fast enough to change Y_e from its initial value (Fuller et al. 2000, Beloborodov 2002b).

For T_0 and $\rho_{b,0}$ typical of GRB outflows, the baryons should initially be in nuclear statistical equilibrium (NSE) consisting predominantly of free protons and neutrons, so the assembly of nuclei always begins from the lightest elements. A key feature of the nuclear reaction network codes implemented here is the inclusion of a large number of reactions involving light, very neutron-rich nuclei (Terasawa et al. 2001, Orito & Iwamoto 2003, in preparation). Besides the well-known paths of $\alpha(\alpha\alpha,\gamma)^{12}$C and $\alpha(\alpha n,\gamma)^{9}Be(\alpha,n)^{12}$C bridging the mass gaps at $A = 4$ and $A = 8$, new reaction channels allowed via these light neutron-rich nuclides have been shown by Terasawa et al. (2001) to critically influence the synthesis of even the heaviest nuclei, especially for expansion with short timescales and/or high neutron excesses. This is indeed the case for our conditions here. Most previous network codes including only a limited number of such reactions would give erroneous results for the present problem. In total, our code used for heavy element synthesis calculations includes over 3000 nuclides, mainly on the neutron-rich side of stability.

On the other hand, we only deal with a limited number of heavy nuclei on the proton-rich side, which, if fully included, may possibly affect the reaction flow when Y_e is near 0.5. We also choose to neglect fission, the detailed physics of which is currently very uncertain (e.g. Cameron 2001), but which may in reality have important consequences for some parameter regimes studied here. These microphysical aspects will be accounted for in subsequent studies (§5). We do include the effects of the increase in temperature and entropy from electron-positron pair annihilation occuring at $T \lesssim$ MeV (e.g. Meyer & Brown 1997).

In some GRB models, strong neutrino irradiation from the central source can also affect the nuclear composition, but this will not be treated here as it is highly model-dependent (see §5). We remark that for all cases under consideration here the neutrons remain kinematically well-coupled to the rest of the fireball plasma throughout the duration of nucleosynthesis (c.f. Derishev, Kocharovsky & Kocharovsky 1999, Fuller et al. 2000).

3. RESULTS AND DISCUSSION

The main parameters in the present problem are L, r_0, η and Y_e. GRB observations put reasonable constraints on L and r_0, so we will keep these to our fiducial numbers of 10^{52} erg s^{-1} and 10^7 cm respectively (hence $kT_0 \simeq 0.93$MeV; see however §5 for the case of collapsars). We thus concentrate on the effect of variations in η and Y_e, for which a wide range of values can be realized. The trajectories are very different for the limiting cases of high and low η. For $\eta = 100$ typical of successful GRBs, $s/k_B \sim 10^5$, and the acceleration phase lasts for $t_s \simeq 1.5$ msec during which T and ρ_b fall extremely rapidly by 2 and 6 orders of magnitude, respectively. The coasting phase here is irrelevant for nucleosynthesis. In comparison, for $\eta = 2$, $s/k \sim 2500$, and the coasting phase is entered at $t_s \simeq 0.23$ msec when T and ρ_b are lower by just factors of 2 and 8, respectively. Much of the reactions can then proceed during the power-law expansion, especially neutron-captures.

Since the production of the more common α and Fe-group elements at intermediate A should be dominated by normal stars and supernovae in the Universe, the signatures of GRB-BRO nucleosynthesis are to be sought in other elements which are not readily synthesized in ordinary stellar environments. We therefore focus our interest here on the light element region of D, Li, Be and B, and on the neutron capture element region much heavier than Fe.

3.1. *Light Elements*

For calculating light element production, a relatively small network limited to nuclei with mass number $A \leq 18$ suffices, as the reaction flow to higher A is not very large. Here we utilize a code developed for big bang nucleosynthesis (BBN), which includes the relevant weak interaction processes and has been extended and updated with reactions for 40 light nuclei in total to study inhomogeneous BBN (Orito & Iwamoto 2003, in preparation). The relative ease of these computations allows us to survey large regions of parameter space.

We first discuss the yields of ^{4}He and D for a wide range of η. These elements can be produced appreciably even in the high η fireballs of successful GRBs (Lemoine 2002, Pruet et al. 2002, Beloborodov 2002), and we extend the regime of consideration down to $\eta = 2$. Like BBN, ^{4}He is the dominant final species besides remaining free nucleons for all cases here, as the majority of the available protons (neutrons) can become locked up in α particles for neutron-rich (proton-rich) conditions.

The left panel of Fig. 1 shows the final abundance of D as contours of constant mass fraction in the η-Y_e parameter plane. For $\eta \gtrsim 20$, the reactions mainly occur during the exponentially expanding acceleration phase. D production depends on $\rho_{b,0} \propto \eta^{-1}$ such that its final abundance is smaller for lower η due to larger reaction flows to ^{4}He, similar to the case of BBN. The production rate is also proportional to $Y_p Y_n \approx Y_e(1-Y_e)$, with a maximum at $Y_e = 0.5$.

Contrastingly, for $\eta \lesssim 10$, the nucleosynthesis proceeds mainly during the coasting phase with power-law expansion, where neutron capture reactions can be active until very late times, $t \lesssim 10^3$ s (see §3.2). Here D synthesis can occur via a novel process: when $Y_e \lesssim 0.5$, free neutrons remain abundant in the outflow until they start decaying into protons, which subsequently can undergo the p(n,γ)d reaction during the latest stages of the expansion. In this regime, D production does not depend strongly on Y_e, as long as $Y_e \lesssim 0.5$. This is an interesting D production mechanism that has not been discussed in previous contexts.

Notable amounts of nuclei with $A > 4$ such as Li, Be and B are created only when $\eta \lesssim 10$. We display the results for ^{11}B in the right panel of Fig. 1 for the range of $\eta = 2-10$. Under neutron-rich conditions ($Y_e \leq 0.5$), ^{11}B is produced by the reaction chains

$$t(\alpha,\gamma)^7\mathrm{Li}(n,\gamma)^8\mathrm{Li}(n,\gamma)^9\mathrm{Li}(\beta)^9\mathrm{Be}(n,\gamma)^{10}\mathrm{Be}(n,\gamma)^{11}\mathrm{B}$$
$$^8\mathrm{Li}(\alpha,n)^{11}\mathrm{B}.$$

In proton-rich environments ($Y_e \geq 0.5$), the main path for ^{11}B production is $^3\mathrm{He}(\alpha,\gamma)^7\mathrm{Be}(\alpha,\gamma)^{11}\mathrm{C}(\beta)$. Other light elements such as ^{6}Li, ^{7}Li and ^{9}Be can also be generated at levels of $X \sim 10^{-8} - 10^{-7}$.

We remark that under certain conditions, light element production may be considerably enhanced through nonthermal reactions such as spallation and/or photodisintegration, but these effects are outside of our present scope (see §5).

3.2. *Heavy Elements*

The synthesis of heavy elements through neutron capture is the focal point of this work. Such processes obviously encompass a vastly larger number of nuclides compared to light element production, so full network calculations are much more cumbersome. Parameter studies with the small, light element network discussed above indicate that the flow to heavy nuclei ($A > 16$) becomes considerable only for $\eta \lesssim 4$. We thus concentrate here only on the most favorable case of $\eta = 2$, and choose selected values for Y_e (< 0.5). Using the full network described in Terasawa et al. (2001), the calculations below have been followed until all reactions have frozen out, typically occurring at $t \sim 10^3$ s.

The $\eta = 2$ outflow is characterized by a very high entropy ($s/k_B \simeq 2500$) and very short initial expansion timescale ($t_{d0} \simeq 0.33$ ms), which can be compared with the values typical of SN neutrino-driven winds (§1). These conditions lead to heavy element synthesis which is markedly different from the usual *r*-process in a number of respects. Displayed in Figure 2 are the final abundances as a function of mass number, for the cases of $Y_e = 0.1$, 0.3, 0.4, 0.48 and 0.498. The abundance patterns are clearly discrepant from the solar distribution, shown here with arbitrary normalization as the uppermost curve. When $Y_e \lesssim 0.4$, implying copious supplies of neutrons, considerable reaction flows can occur to high mass numbers, ending up in large fractions of the heavier nuclei. However, we also see that the abundances are at levels of $Y \simeq 10^{-6}$ even at the peaks, which is quite low compared to the SN wind *r*-process. This is due to the combination of small t_{d0}, which limits the initial, charged particle reaction flow at small A, and the low density, which hinders the subsequent neutron capture flow to higher A. Note that the apparent abundance peak at $A \simeq 250$ is an artifact of our neglect of fission and results from artificial pileup at the limit of our reaction network. In situations where this peak becomes dominant, the realistic effects of fission (and possible consequent fission cycling) may significantly affect the final abundance pattern (§5). For $Y_e = 0.48$ and 0.498, the flows to high mass nuclei are drastically reduced due to the low neutron excess, and only small amounts of elements result at $A \lesssim 50$ and $A \lesssim 20$, respectively.

Our abundance distributions for $Y_e \lesssim 0.4$ show three peaks around $A \simeq$87, 135 and 205 located in between the solar *s*- and *r*-process peaks. This is a clear manifestation of nuclei with neutron magic numbers forming on a reaction flow path intermediate between those of the *s*- and *r*-processes. Figure 3 shows a snapshot of the calculated reaction flow in the *N*-*Z* plane for the case of $Y_e = 0.3$, at $t \simeq 4.2$ s when the density has fallen to 1.2×10^{-4} g cm^{-3}. Due to the low density in the outflow, the neutron capture rates are too low to effectively establish (n, γ)-(γ, n) equilibrium, even when the neutrons constitute a major fraction of the baryons. Instead, as ρ_b and T decrease steadily in the coasting phase, β-decays begin to compete with the neutron capture reactions, leading to a flow path that gradually evolves in time from near the dripline (*r*-process-like) to that near the β-stability line (*s*-process-like).

We also note that the differences in the abundances between the peak and interpeak elements are larger than that of the solar pattern. This is due to the fact that nuclei in the moderately neutron-rich region have longer β-decay lifetimes than compared to those near the dripline. Therefore, reaction flows at the magic nuclei are halted for a longer time, resulting in larger peak-to-interpeak contrasts.

A final point is that the low density here keeps the neutrons from ever being exhausted by neutron capture, in contrast to the *r*-process in SNe. Instead the neutrons remain abundant after the capture reactions freeze out until they freely decay into protons.

Neutron capture nucleosynthesis in environments with low neutron abundances, where the flow path is determined by the balance of neutron captures and β-decays rather than (n,γ)-(γ,n) equilibrium, has been discussed previously by Blake & Schramm (1976) and Blake et al. (1981) and christened the "n-process". Our physical conditions are quite different from those considered by the above authors, in that we have a very large neutron abundance yet a low total density. However, the basic physical processes are similar. BROs associated with GRBs are therefore natural astrophysical sites for operation of the *n*-process.

4. OBSERVATIONAL IMPLICATIONS

The calculations presented above are based on a number of simplifications, so they should be regarded as tentative expectations from nucleosynthesis in actual GRB-BROs (although they may be fair representations of BROs in neutron star mergers or supranovae, §2). Various realistic physical effects can modify these results in important ways (§5). Nevertheless, some qualitative trends seen here should remain generally valid. Below we discuss the observational implications of GRB-BRO nucleosynthesis, taking at face value the results of our $\eta = 2$, mildly relativistic fireball as a fiducial case. These considerations should also serve as a reference point when more detailed predictions become available in the future.

Since it was found that GRB-BROs can be interesting sites of neutron capture nucleosynthesis, the first important comparison we can make is between the heavy element yields from a single GRB-BRO event and that expected from a normal core collapse SN. For neutrino-driven wind models of SNe, the typical abundance of r-process peak elements in the ejecta is $Y_{SN\nu} \sim 10^{-4}$ and the total ejecta mass should be $M_{SN\nu} \sim 10^{-5}$-$10^{-4}\mathrm{M}_\odot$ (e.g. Meyer 1994, Terasawa 2002). To be compared are the BRO final abundances for the realistic range of $Y_e \simeq 0.1-0.4$, where the peak abundance is $Y_{BRO} \sim 10^{-6}$ (Fig.2), and the total ejecta mass can be of order $M_{BRO} \sim 10^{-3}$-$10^{-2}\mathrm{M}_\odot$. [2] This gives a total heavy element yield per GRB-BRO event comparable to SNe, albeit with large uncertainties.

As a first guess, the contribution of GRB-BROs to the solar/Galactic abundances then is a matter of event rates compared to SNe, if SNe are in fact the main sources of the solar r-process elements. The intrinsic, beaming-corrected event rates for successful GRBs are estimated to be $R_{GRB} \sim 10^{-5}$-$10^{-4}\mathrm{yr}^{-1}$ (e.g. Frail et al. 2001), which is $\sim$ 0.1 - 1 % of the SN rate $R_{SN} \sim 10^{-2}\mathrm{yr}^{-1}$. If a BRO with the above parameters is associated with every GRB as a circum-jet wind, then the nominal allowance of GRB-BROs to the solar abundances is $\sim$ 0.1 - 1 %. If failed GRBs with similar properties occur at a higher rate, the contribution will be even greater. However, we must remember that the abundance patterns arising from our fiducial outflow are different from solar, particularly the location of the peaks. In order to avoid overproduction of the elements between the solar r- and s-peaks, the true contribution may be even less. At the very least, such GRB-BROs may be the origin of select rare elements not easily produced under any other conditions (see e.g. Blake et al. 1981). Alternatively, some realistic effects discussed in §5 may alter the nucleosynthesis in GRB-BROs so as to make them potential sources of the solar r-process elements.

Even if GRB-BROs hold a minor share of the solar abundances, some observable environments may directly manifest the local abundance pattern of the BRO ejecta. Detailed spectroscopic observations of metal-poor stars with metallicities down to [Fe/H] $\sim$ -3 have so far shown abundance patterns very similar to that of the solar r-process for elements with $56 \leq Z \lesssim 70$, at least for the so-called r-process enhanced stars (e.g. Truran et al. 2002 and references therein). This fact, together with the observed large scatter in the r-process abundances, indicate that chemical evolution in the early Galaxy proceeded very inhomogeneously, and the abundance patterns in metal-poor stars are set mainly by individual SN explosions of the previous stellar generation (Audouze & Silk 1995, Shigeyama & Tsujimoto 1998). If GRBs are associated with the most massive range of progenitor stars, these explosions may have dominated in the earliest stages of the Galaxy, so that their nucleosynthesis products can be discerned in metal-poor stars with the lowest metallicities. We can estimate the total mass of gas swept up by a GRB-BRO and with which the BRO ejecta mixes to be $M_{sh} \sim 3 \times (10^4$-$10^5)\mathrm{M}_\odot$ (Shigeyama & Tsujimoto 1998). The dilution factor per event is then $f_{MPS} = M_{BRO}/M_{sh} \sim 10^{-7.5}$, and the expected heavy element abundance is $Y_{MPS} \sim f_{MPS} Y_{BRO} \sim 10^{-13.5}$ or roughly 2.5 dex below solar, an observable level. It is intriguing to see if future observations of extremely metal-poor stars (e.g. Christlieb et al. 2002) reveal a heavy element abundance pattern distinct from that of the solar r-process.

Another interesting locale is the companion star in a black hole binary system, where the explosive event that formed the black hole may have left traces of the explosion ejecta on the surface of the companion. (This argument excludes neutron star merger scenarios.) Indeed, observations of the black hole binary GRO J1655-40 (Nova Sco) have uncovered anomalous α-element enhancements indicating contamination by supernova ejecta, possibly of the energetic “hypernova” variety (Israelian et al. 1999, Podsiadlowski et al. 2002). Very crudely, the fraction of the BRO ejecta captured by the companion may be $f_{cap} \sim 10^{-3}$, considering a typical solid angle subtended by the star. The mass of the mixing zone between the ejecta and the companion surface could be in the range $M_{mix} \sim 10^{-4}-10^{-2}\mathrm{M}_\odot$ (Israelian et al. 1999, Qian 2000), so that the dilution factor here is $f_{bin} \sim f_{cap} M_{BRO}/M_{mix} \sim 10^{-4}-10^{-1}$, although these values are very uncertain. This leads to $Y_{bin} \sim f_{bin} Y_{BRO} \sim 10^{-10}-10^{-7}$, which is a staggeringly high overabundance with respect to solar $Y_\odot \sim 10^{-11}$, and should be clearly detectable. High resolution spectroscopic observations of such stars are warranted to search for neutron-capture elements and study their detailed abundance patterns.

In discerning light element products from BROs, the only hope is offered by the black hole binary companions, as their contribution to the solar abundances and even very metal-poor stars can be shown to be miniscule. Taking the $\eta = 2$ case, we will be most optimistic and assume the least dilution $f_{bin} \sim 10^{-1}$, and also select Y_e where the maximum final abundance is achieved for each element. For D, ^{7}Li, ^{6}Li, ^{9}Be and ^{11}B, respectively, these are $Y_e \sim$ 0.1, 0.7, 0.5, 0.4 and 0.1, at which the abundance by number on the companion surface would be $Y_{bin} \sim 10^{-3}, 2 \times 10^{-8}, 10^{-10}, 10^{-10}$ and 4×10^{-8}. This must be compared to the solar abundances for the respective elements, $Y_\odot \sim 4 \times 10^{-5}, 10^{-8}, 6 \times 10^{-10}, 10^{-10}$ and 10^{-9}. Overabundance is expected to be high only for D, and is marginal for ^{7}Li and ^{11}B. More dilution or deviations from the optimal Y_e, as well as stellar depletion effects that can be severe for D, would render them difficult to observe, if at all. However, light element production may become more prolific for BROs which are non-relativistic and/or collimated, or when circumstances allow for significant spallation (§5).

Either in extremely metal-poor stars or in black hole binary companions, observations of the pure ejecta abundance pattern may provide us with valuable insight into the origin of GRBs. It is evident in Figs.1 and 2 that the final abundance patterns of both the light and heavy elements are quite sensitive to Y_e, which in turn implies that observations can significantly con-

[2] Note that for $\eta \sim 2$, $M_{BRO} \sim 10^{-2}\mathrm{M}_\odot$ implies a total outflow energy $E_{BRO} \sim 4 \times 10^{52}$erg. This would be consistent with $L_{52} = 1$ if, for example, the GRB duration is $\Delta t \sim 10$s and the BRO is mildly collimated into a fraction $f_\Omega \sim 0.4$ of the sky. Although this BRO energy is larger than the inferred intrinsic (i.e. beaming-corrected) total energies for GRB jets, $E_{GRB} \sim 10^{51}$erg (Frail et al. 2001), such values may not be so unreasonable from certain physical viewpoints (e.g. Levinson & Eichler 2000), and is also concordant with the observed energetics of “hypernovae”, which may possibly correspond to failed GRBs.

strain its value. Since Y_e is an important quantity characterizing the nature and conditions of the central engine, the nucleosynthetic products can shed light on the innermost regions of GRB sources, which are otherwise very difficult to probe.

5. CONCLUSIONS AND FURTHER PROSPECTS

The salient points of this work are summarized. We have explored the possibility of nucleosynthesis in baryon-rich outflows that are expected to accompany GRBs. Detailed reaction network calculations were performed in the context of the fireball model with varying baryon load. It was found that mildly relativistic outflows can synthesize appreciable quantities of heavy neutron capture elements with masses up to the actinides via the "n-process", as well as interesting amounts of light elements such as deuterium. Their characteristic abundance patterns may be discernible in black hole binary companion stars or in extremely metal-poor stars, possibly offering important information on the GRB central engine conditions. Some contribution to the solar heavy element abundances may also exist.

We now give brief discussions of various effects that have not been accounted for in this work, but in reality can significantly influence the outcome of GRB-BRO nucleosynthesis. These possibilities point us toward a variety of subsequent studies.

In our reaction network calculations, fission was not included for the sake of simplicity. However, we saw that for a plausible range of Y_e the reaction flow can extend well into the actinide region where fission should be an unavoidable process. Since the free neutrons in our BROs are always far from being exhausted and stay abundant until very late times (§3.2), a highly probable consequence is fission cycling, whereby fission products act as seed nuclei for successive cycles of reaction flows into the fission regime. This should affect the resulting heavy element abundances in interesting ways and is currently under investigation (Terasawa et al., in preparation). Another facet not included in our reaction network is heavy nuclei in the proton-rich region, which should be important for situations when $Y_e \gtrsim 0.5$ and may potentially give rise to p-process nuclei (Iwamoto et al., in preparation).

Our dynamical framework here was limited to the basic spherical fireball model. Although the BROs may not be as strongly collimated as the GRB jets, some degree of collimation (e.g. through external gas pressure gradients or magnetic stresses) is naturally expected, causing modifications in the density and temperature trajectories. While the details are model-dependent, collimation should generally tend to prolong the phase of initial expansion when the charged particle reactions mainly proceed (Lemoine 2002, Beloborodov 2002b). This would permit the initial reaction flow to reach larger A, resulting in increased heavy element production for cases with high neutron excess, as well as larger light element yields.

For reasons discussed in §2, we had also restricted the dimensionless entropy to $\eta \gtrsim 2$, meaning that the outflows are at least mildly relativistic and the total baryon masses are $M_b \lesssim 2.8 \times 10^{-2} M_\odot E_{53}$. However, much larger baryon loading can conceivably happen in some GRB scenarios like collapsars, leading to BROs in the nonrelativistic regime. These should be even more efficient nucleosynthetic cauldrons, as they involve a lower entropy, longer initial expansion time, and larger total ejecta mass. In fact, the effects of nonrelativistic baryon loading (and to a lesser extent, collimation) may allow the realization of physical conditions that are ideal for reproducing the solar r-process abundances. This important prospect of GRB-BROs as potential r-process sites is worth exploring in some detail.

Another significant, albeit model-dependent process is neutrino irradiation of the BRO from a central source. Strong thermal neutrino emission is expected in many types of GRB progenitors, including core collapse and neutron star merger models. This can impact the nucleosynthesis in different ways, either through its thermal and dynamical effects on the BRO expansion, or through neutrino-induced interactions on the nucleons and nuclei (e.g. Meyer 1995).

The considerable fraction of free neutrons remaining after BRO nucleosynthesis (§3.2) may induce a host of noteworthy effects before they decay into protons at a radius $r_n \sim 3 \times 10^{13}\mathrm{cm}\Gamma$. For nucleosynthesis, an intriguing possibility is the operation of an "external" neutron capture process, i.e. heavy element synthesis by capture of the BRO neutrons on any external baryonic matter with which the outflow interacts and mixes, especially when the BRO is nonrelativistic. The external material may be the outlying stellar wind of the progenitor star, the surface of a binary companion, or the overlying stellar envelope in the case of a collapsar (Pruet et al. 2002b). Such processes may be externally seeded, as any nuclei like Fe preexisting in the environs can constitute the seed for neutron captures. Further interesting consequences of neutrons can be caused by their kinematic decoupling from the rest of the fireball plasma, such as modifications to the dynamical evolution of the fireball and/or blastwave (e.g. Derishev et al. 1999, Fuller et al. 2000, Beloborodov 2002a), characteristic neutrino and gamma-ray signatures (Bahcall & Mészáros 2000, Mészáros & Rees 2000), and production of light elements by spallation (Pruet et al. 2002a; see below).

Although we only dealt with thermal nuclear reactions in the expanding BRO, additional, nonthermal nuclear processes can alter the nuclear composition in different ways in real GRB-BROs. These may actually dominate the production of some elements, particularly D, Li, Be and B. For the high Γ GRB jets, the observed short timescale variability of the GRB emission may entail substantial fluctuations and dissipation by internal shocks within the outflow, which can lead to spallation of ^{4}He and other existing nuclei (Beloborodov 2002b). [3] Appreciable spallation may also be induced by interaction of the outflow with external matter (e.g. progenitor stellar wind, binary companion star, massive star envelope), affecting both the nuclei inside the BRO and those composing the external baryons. Under circumstances where free neutrons become kinematically decoupled, bulk motions relative to the rest of the flow may develop and induce spallation by neutrons, either internally or externally (Pruet et al. 2002a, Beloborodov 2002b). [4] Photodisintegration by nonthermal gamma-rays emitted in internal shocks can also take place outside the photosphere (Lemoine 2002), although this may not be so significant for BROs due to their large photospheric radii.

One particular setting where virtually all of the above effects (plus some other unique ones) can be essential is the collapsar scenario, in which the GRB jet and associated BRO first propagate through the dense envelope of a massive star be-

[3] This effect is probably less important for the low Γ BROs studied here, since they may not be as strongly time-varying as GRB jets, and also because internal shocks in the BROs would occur at much smaller radii where the temperature is still high and the outflow optically thick.

[4] In our BROs, however, coupling of the neutrons to the rest of the plasma through elastic n-p collisions generally persist until late times.

fore emerging and generating a GRB (MacFadyen & Woosley 1999). There is a multitude of deviations from the simple fireball picture due to the strong outflow-star interaction, such as reverse shock heating of the flow, expansion of the shocked material into a cocoon, entrainment and mixing with the stellar material through instabilities, breakout from the envelope and ensuing lateral expansion, etc (Mészáros & Rees 2001, Zhang et al. 2002, Aloy et al. 2002, Ramirez-Ruiz et al. 2002). In fact, the expansion timescale at envelope breakout (radii $r \sim 10^{11}$cm) may be more important for nucleosynthesis than the expansion timescale at the central engine (see discussion in Pruet et al. 2002a). Quantitative modeling of nucleosynthesis within this complicated picture is a very interesting but challenging goal.

The ultimate answer to the problem of GRB-BRO nucleosynthesis is contingent on elucidating the physics of the GRB central engine, including the progenitor's identity, the central engine configuration and the outflow formation mechanism, from which we may be a long way. Nevertheless, we may hope to build increasingly realistic models, adding step by step different levels of complexity. Comparison of such calculations to observations of various sites may then allow us to constrain the unknown properties of the GRB source, as well as to clarify the role of GRB-BROs in the chemical evolution of the Galaxy. Further investigations of GRB-BRO nucleosynthesis in various directions should provide us with a rich scope of interesting work for the future.

We are grateful to S. Woosley, G. Mathews, B. Meyer, H.-T. Janka, W. Hillebrandt and C. Travaglio for fruitful discussions. T. Sasaqui is thanked for his help in the early stages of this study. One of the authors (M. T.) wishes to acknowledge the fellowship of the Japan Society for Promotion of Science (JSPS).

REFERENCES

Audouze, J, & Silk, J. 1995, ApJ, 451, L49
Aloy, M.-A., Ibanez, J.-M., Miralles, J.-A. & Urpin, V. 2002, A&A, submitted (astro-ph/0209575)
Bahcall, J. N. & Mészáros, P. 2000, Phys. Rev. Lett., 85, 1362
Beloborodov, A. M. 2002a, ApJ, submitted (astro-ph/0209228)
Beloborodov, A. M. 2002b, ApJ, submitted (astro-ph/0210522)
Blake, J. B. & Schramm, D. N. 1976, ApJ, 209, 846
Blake, J. B., Woosley, S. E., Weaver, T. A. & Schramm, D. N. 1981, ApJ, 248, 315
Cameron, A. G. W. 2001, ApJ, 562, 456
Christlieb, N. et al. 2002, Nature, 419, 904
Derishev, E. V., Kocharovsky, V. V. & Kocharovsky, V. Vl. 1999, ApJ, 521, 640
Frail, D. et al. 2001, ApJ, 562, L55
Fuller, G. M., Pruet, J. & Abazajian, K. 2000, Phys. Rev. Lett., 85, 2673
Heise, J., in't Zand, J., Kippen, R. M. & Woods, P. M. 2001, astro-ph/0111246
Huang, Y. F., Dai, Z. G. & Lu, T. 2002, MNRAS, 332, 735
Israelian, G., Rebolo, R., Basri, G., Casares, J. & Martin, E. L. 1999, Nature, 401, 142
Janka, H.-T. & Ruffert, M. 2001 (astro-ph/0101357)
Kippen, R. M. et al. 2002, astro-ph/0203114
Lemoine, M. 2002, A&A, 390, L31
Levinson, A. & Eichler, D. 1993, ApJ, 418, 386
Levinson, A. & Eichler, D. 2000, Phys. Rev. Lett., 85, 236
MacFadyen, A. I. & Woosley, S. E. 1999, ApJ, 524, 262
Mészáros, P. 2002, ARA&A, 40, 137
Mészáros, P. & Rees, M. J. 2000, ApJ, 541, L5
Mészáros, P. & Rees, M. J. 2001, ApJ, 556, L37
Meyer, B. S. 1994, ARA&A, 32, 153
Meyer, B. S. 1995, ApJ, 449, L55
Meyer, B. S. & Brown, J. S. 1997, ApJS, 112, 199
Meyer, B. S. 2002, Phys. Rev. C, submitted (astro-ph/0207227)
Narayan, R., Piran, T. & Kumar, P. 2001, ApJ, 557, 949
Nomoto, K. et al. 2002, astro-ph/0209064
Paczyński, B. 1986, ApJ, 308, L43
Paczyński, B. 1990, ApJ, 363, 218
Piran, T. 1999, Phys. Rep.
Podsiadlowski, P. et al. 2002, ApJ, 567, 491
Pruet, J., Abazajian, K. & Fuller, G. M. 2001, Phys. Rev. D, 64, 063002
Pruet, J., Guiles, S. and Fuller, G. M. 2002a, ApJ, 580, 368
Pruet, J., Woosley, S. E. & Hoffman, R. D. 2002b, ApJ, submitted (astro-ph/0209412)
Qian, Y.-Z. 2000, ApJ, 534, L67
Ramirez-Ruiz, E., Celotti, A. & Rees, M. J. 2002, MNRAS, 337, 1349
Rhoads, J. E. 2001, astro-ph/0103028
Rossi, E., Lazzati, D. & Rees, M. J. 2002, MNRAS, 332, 945
Rosswog, S. & Ramirez-Ruiz, E. 2002, MNRAS, 336, L7
Shigeyama, T. & Tsujimoto, T. 1998, ApJ, 507, L135
Takahashi, K., Witti, J. & Janka, H.-T. 1994, A&A, 286, 857
Terasawa, M., Sumiyoshi, K., Kajino, T., Mathews, G. J. & Tanihata, I. 2001, ApJ, 562, 470
Terasawa, M. 2002, Ph.D. Thesis, University of Tokyo
Terasawa, M., Sumiyoshi, K., Yamada, S., Suzuki, H. & Kajino, T. 2002, ApJ, 587, L137
Truran, J. W., Cowan, J. J., Pilachowski, C. A. & Sneden, C. 2002, PASP, 114, 1293
Vietri, M. & Stella, L. 1998, ApJ, 507, L45
Woosley, S. E., Wilson, J. R., Mathews, G. J., Hoffman, R. D. & Meyer, B. S. 1994, ApJ, 433, 229
Woosley, S. E., Zhang, W. & Heger, A. 2002a, astro-ph/0206004
Woosley, S. E., Zhang, W. & Heger, A. 2002b, astro-ph/0211063
Zhang, B. & Mészáros, P. 2002, ApJ, 571, 876
Zhang, W., Woosley, S. E. & MacFadyen, A. I. 2002, ApJ, accepted (astro-ph/0207436)

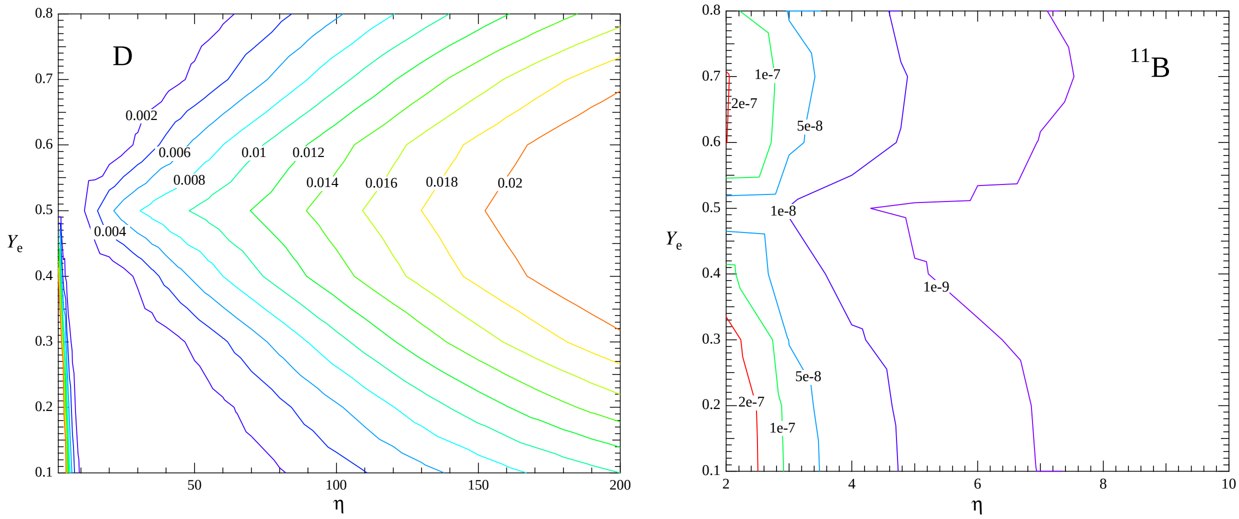

FIG. 1.— Contours of the final abundances by mass fraction of deuterium (left panel) and boron (right panel) for different parameter values of η and Y_e.

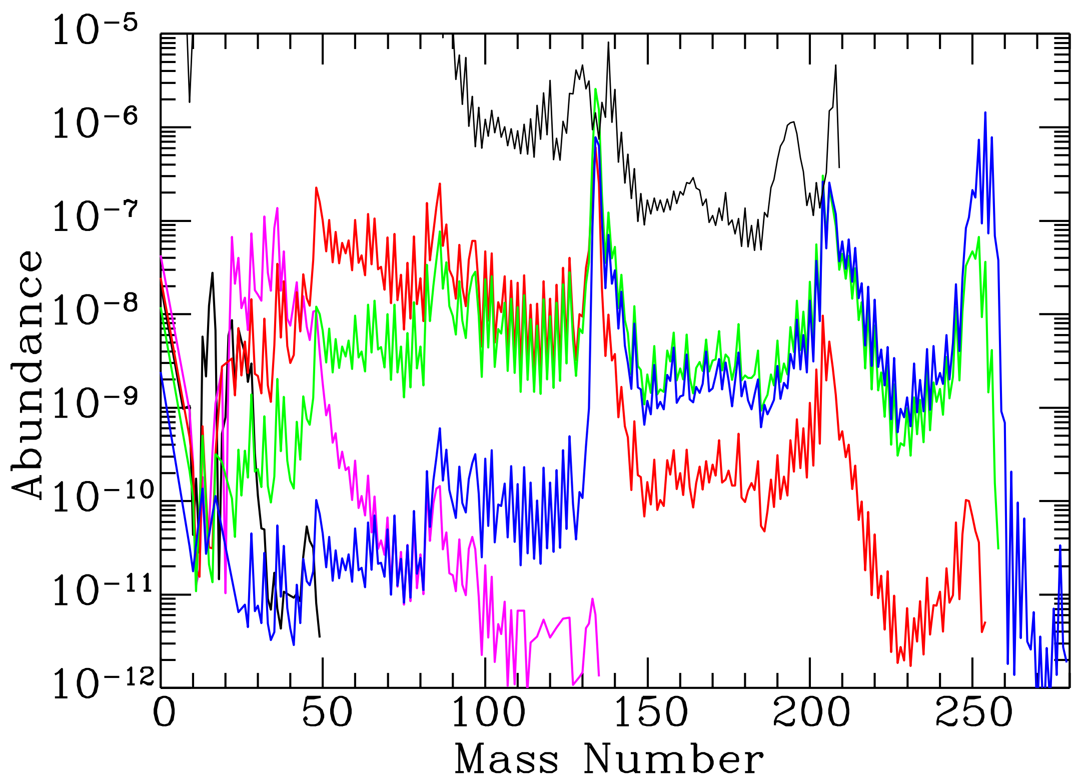

FIG. 2.— Final abundances for different Y_e as a function of mass number. The results for Y_e = 0.1, 0.3, 0.4, 0.48 and 0.498 are represented by the blue, green, red, purple and black curves, respectively. The solar abundance distribution in arbitrary units is shown by the uppermost black curve.

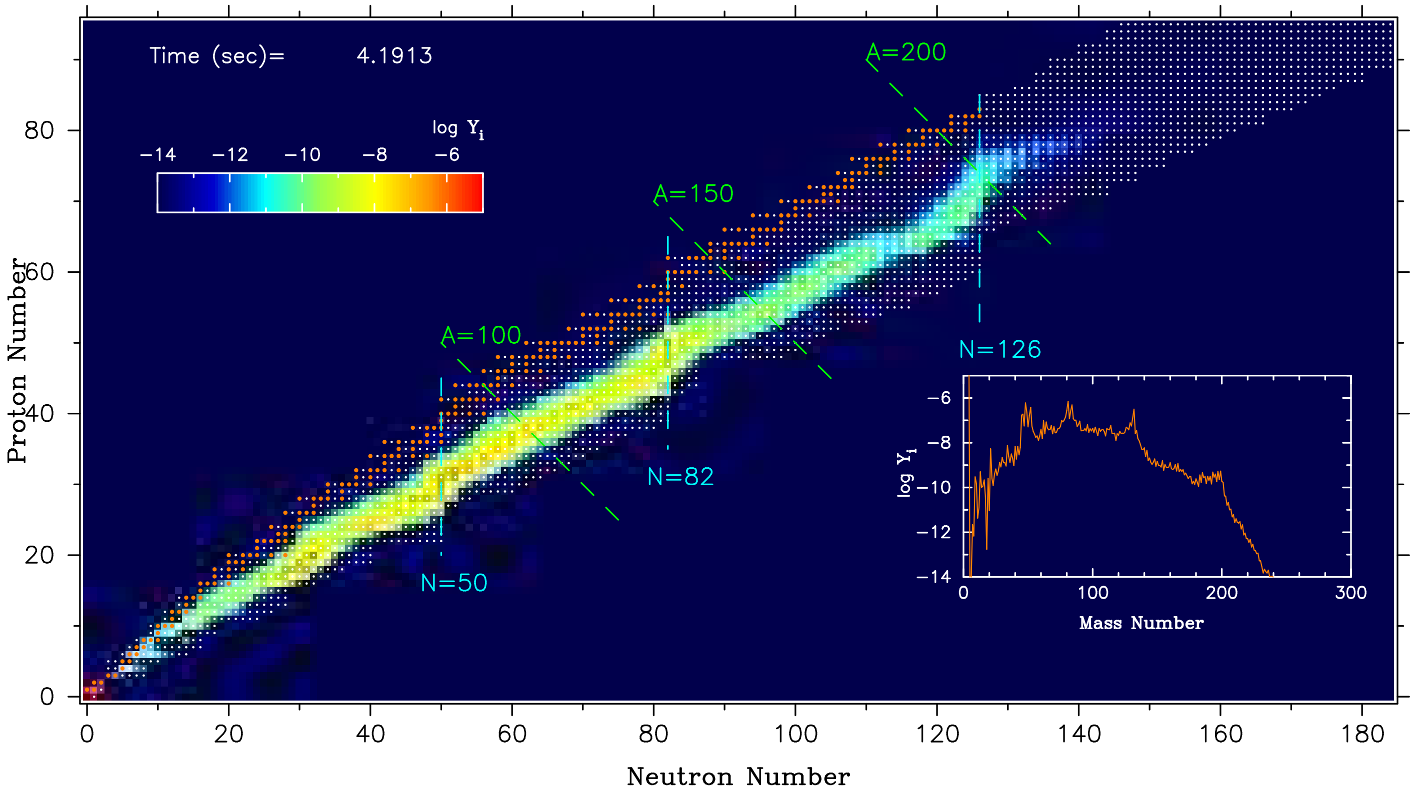

FIG. 3.— Snapshot of the reaction flow in the plane of neutron number N versus proton number Z for the case of Y_e = 0.3, at time $t \simeq 4.2$ s and density $\rho_b \simeq 1.2 \times 10^{-4}$ g cm^{-3}. The orange and white circles indicate stable and unstable nuclei, respectively. The inset shows the number fraction Y of heavy elements as a function of mass number A.